

See discussions, stats, and author profiles for this publication at: <https://www.researchgate.net/publication/263943322>

Experiments and Kinetic Modeling for CO₂ Gasification of Indian Coal Chars in the Context of Underground Coal Gasification

ARTICLE *in* INDUSTRIAL & ENGINEERING CHEMISTRY RESEARCH · NOVEMBER 2012

Impact Factor: 2.59 · DOI: 10.1021/ie3022434

CITATIONS

12

READS

84

7 AUTHORS, INCLUDING:



Sateesh Daggupati

Reliance Industries Limited

11 PUBLICATIONS 70 CITATIONS

[SEE PROFILE](#)



Sanjay Madhusudan Mahajani

Indian Institute of Technology Bombay

123 PUBLICATIONS 1,392 CITATIONS

[SEE PROFILE](#)



Preeti Aghalayam

Indian Institute of Technology Madras

37 PUBLICATIONS 636 CITATIONS

[SEE PROFILE](#)



Anuradha Ganesh

indian institute of technology, Bombay

44 PUBLICATIONS 1,358 CITATIONS

[SEE PROFILE](#)

Experiments and Kinetic Modeling for CO₂ Gasification of Indian Coal Chars in the Context of Underground Coal Gasification

Ramesh Naidu Mandapati,[†] Sateesh Daggupati,[†] Sanjay M. Mahajani,[†] Preeti Aghalayam,[§] Rajender K. Sapru,^{||} Rakesh K. Sharma,^{||} and Anuradha Ganesh*,[‡]

[†]Department of Chemical Engineering and [‡]Department of Energy Science and Engineering, IIT Bombay, Powai, Mumbai-400076, India

[§]Department of Chemical Engineering, IIT Madras, Chennai-600036, India

^{||}UCG Group, IRS, ONGC, Chandkheda, Ahmedabad-380005, Gujarat, India

ABSTRACT: Gasification of four Indian coals is carried out in a CO₂ atmosphere, using a thermogravimetric analyzer (TGA) to determine the intrinsic kinetics over a temperature range of 800–1050 °C with different partial pressures of CO₂. The applicability of three models, viz., the volumetric reaction model, the shrinking core model and the random pore model, is evaluated. Of these three models, the random pore model is found to be the most suitable for all the coals considered in the current study. The dependence of the reaction rate on the gas-phase partial pressures is explained by the Langmuir–Hinshelwood model, and the parameters for the inhibition due to CO and CO₂ are determined by performing experiments at different partial pressures. In underground coal gasification, the reaction takes place on reasonably large sized coal particles, wherein diffusion effects are significant. A one-dimensional reaction diffusion model is therefore developed in order to determine the diffusional resistance in the coal particle, and values of diffusivity are estimated.

1. INTRODUCTION

Coal is widely used for the production of power, and most of the power plants are based on combustion processes. These power plants are mainly responsible for the emissions of carbon to the environment. To reduce the carbon emissions, clean coal technologies like integrated gasification combined cycle (IGCC)^{1,2} and underground coal gasification (UCG)³ are considered to be the promising options worldwide. The synthesis gas (syngas) from these gasification processes can be used for generating power or synthesizing liquid fuels and chemicals. The gasification process is associated with a number of solid–gas reactions, including combustion, steam and CO₂ gasification, and gas-phase reactions such as the water gas shift reaction and combustion of released pyrolysis gases. Some of these reactions are kinetically controlled, while the others are governed by reaction thermodynamics. Understanding the kinetics of several reactions is therefore essential for the efficient and reliable design of the coal gasification systems. Gasification kinetics is generally studied in the laboratory using fluidized beds, fixed beds, drop tube furnaces, wire mesh reactors, and thermogravimetric analyzers (TGA). Of these, the TGA is a widely used because of its simplicity of design and ease of operation.⁴

In UCG, combustion of coal is the main source of energy used to enhance the rate of gasification reactions. The main product of this exothermic reaction is CO₂, which also acts as a gasifying agent. UCG may be performed using either steam and oxygen or only oxygen as reactant gas(es). In the latter case, the operating temperature is relatively high (>800 °C) and gasification is mainly due to the reaction of the coal with the carbon dioxide (eq 1), whereas in the former case, gasification with steam is also an important reaction. Gasification of coal in general and the reaction of CO₂ with coal/char in particular are important in

both surface gasification processes, such as IGCC, and underground coal gasification.



Many researchers have investigated the CO₂ gasification reaction of char derived from biomass and coal. The reactivity of the coal char is found to depend on the rank of coal^{5–8} and mineral matter. Generally, lower ranked coals have higher reactivity as compared to the high-rank coals.^{5,6} Group VIII metals as well as alkali and alkaline earth catalysts are effective catalysts for gasification^{9–12} at low temperatures. For low-rank coals, mineral matter naturally present in the coal acts as a catalyst.^{13–19} As expected, the rate of gasification depends on the pressure as well. At low to moderate pressures, an increase in pressure increases the rate of gasification before the effect diminishes at high pressures.^{20–22} The observed dependence of the gasification rate on pressure varies from zero- to first-order based on the type of coal.^{23–27}

Different models have been reported to explain the kinetics of CO₂ gasification.⁴ These models are summarized in Table 1. Among these, the models widely used by researchers are the volumetric reaction model, the shrinking core model, the modified volumetric model, and the random pore model. In the present work, we first experimentally investigate the intrinsic kinetics of CO₂ gasification using a thermogravimetric analyzer. The applicability of each model is examined. The presence of CO is known to inhibit the CO₂ gasification of char. Hence, the kinetics of the CO₂ gasification in the presence of CO is

Received: August 23, 2012

Revised: September 25, 2012

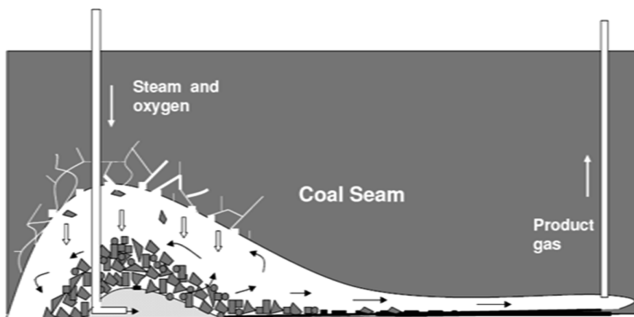
Accepted: October 8, 2012

Published: October 8, 2012

Table 1. Summary of Models for Gasification Kinetics

model	governing equation	remarks	ref
volumetric reaction model	$\frac{dx}{dt} = k(1-x)$	reaction takes place in the entire volume	Levenspiel ²⁸
shrinking core model	$\frac{dx}{dt} = k(1-x)^{2/3}$	reaction takes place on the surface and the particle shrinks as the reaction progresses	Levenspiel ²⁹
random capillary model	$\frac{dx}{dt} = 4\pi(1-x)\sqrt{A_1^2 + A_0 \ln(1-x)}$	A_1 and A_2 are empirical constants	George et al. ³⁰
random pore model	$\frac{dx}{dt} = k(1-x)\sqrt{1 - \Psi \ln(1-x)}$	Ψ is a structural parameter	Bhatia et al. ³¹
discrete random pore model	$\frac{dx}{dt} = k(1-x)(1+\alpha)\sqrt{1 - \Psi_E \ln(1-x)}$	Ψ_E is the effective structural parameter and α is a discreteness parameter	Bhatia et al. ³³
modified discrete random pore model	$\frac{dx}{dt} = \frac{\exp(-V_{\mu E})}{(1-\epsilon_{\mu 0})} \left\{ \sigma S_{\mu E 0} \frac{d\bar{n}}{dt} + \pi \sigma^2 L_{\mu E 0} \frac{d\bar{n}^2}{dt} \right\}$	takes into account different initial surface reactivity	Srinivasulu et al. ³⁴
modified volumetric model	$\frac{dx}{dt} = a^{1/b} b(1-x)[- \ln(1-x)]^{b-1/b}$	a and b are empirical constants	Kasoaka et al. ³⁵
Dutta and Wen model	$\frac{dx}{dt} = aKC_g(1-x)$ $a = 1 \pm x^{\nu\beta} \exp(-\beta x)$	a is the ratio between the available surface area and the initial surface area per unit weight	Dutta et al. ³⁶
Johnson model	$\frac{dx}{dt} = f_1 k(1-x)^{2/3} \exp(-\alpha x^2)$	f_1 is the relative reactive factor and αx^2 is the influence of the effective surface area	Anil et al. ³⁷
unification theory model	grain model, random pore model, and any model can be applied	when conversion is plotted against dimensionless time $\tau = (t/t_{0.5})$, all gasification data falls on a single master curve up to conversion levels <70%	Raghunathan et al. ³⁸

determined using a Langmuir–Hinshelwood formulation. The UCG process (Figure 1) is different from surface gasification in

Figure 1. Schematic diagram of the UCG process.³⁹

the sense that the reaction takes place over a coal particle of reasonably large size (few centimeters). In this case, the diffusional resistance offered by the particle plays an important role and influences the overall rate of reaction. Thus, in this work, along with intrinsic kinetics, we also bring out the importance of the associated diffusion effects and model them with reasonably good accuracy.

2. EXPERIMENTAL SECTION

In this work, all the experiments are performed over char particles, which are obtained by pyrolyzing coal separately, prior to the start of the experiments. We feel that it is important to understand the gasification of chars in the context of underground coal gasification. In UCG, the underground reactions involve pyrolysis of the coal surface at a lower temperature prior to exposure to the gasification environment. Hence, all the experiments in this work pertain to the reactive properties of char, which is prepared as explained below.

2.1. Char Preparation. The char used in the present studies is prepared from four different Indian coals. The sources and properties of these coals are given in Table 2. The coal is dried at 30 °C and crushed to a size between 2 and 3 mm. Char is separately prepared in a quartz tube reactor under an inert atmosphere of nitrogen. Initially, the coal sample is kept at 110 °C for 1 h to remove the moisture content of the coal and to flush out the air present in the reactor. The temperature is then increased to 950 °C at a rate of 30 °C/min and maintained at that temperature for a sufficiently long time until the entire volatile matter is released. Outlet gases are continuously analyzed using a gas chromatograph. The composition of these gases informs us of the completion of the pyrolysis reaction. The obtained char is

Table 2. Proximate and Ultimate Analysis (dry basis) of the Coal Samples

	coal type source	coal A (lignite) GIPCL, India	coal B (sub-bituminous) Western Coalfields Ltd.	coal C (sub-bituminous) Singareni Collieries Co.	coal D (sub-bituminous) Mahanadi Coalfields Ltd.
proximate analysis	volatile matter (%)	44.92	8.79	13.8	20.34
	fixed carbon (%)	46.61	68.29	58.54	43.93
	ash (%)	8.47	22.91	27.66	35.73
ultimate analysis	carbon (%)	59.77	37.32	55.84	49.42
	hydrogen (%)	4.92	3.38	4.02	2.58
	nitrogen (%)	1.1	1.0	0.04	0
	oxygen (%)	26.65	5.76	6.55	4.15

Table 3. Composition of the Ash Obtained from Different Coal Samples

compd (wt %)	coal A	coal B	coal C	coal D
CaO	34.16	4.31	2.85	3.45
Fe ₂ O ₃	7.6	0.11	1.10	2.65
K ₂ O	0.06	0.84	0.54	0.80
MnO	0.07	0.07	0.04	0.04
P ₂ O ₅	0.01	0.04	1.13	0.77
SO ₃	10.71	0.44	0.74	1.14
SrO	0.13	0.05	0.14	0.07
TiO ₂	0.37	1.70	1.53	1.83

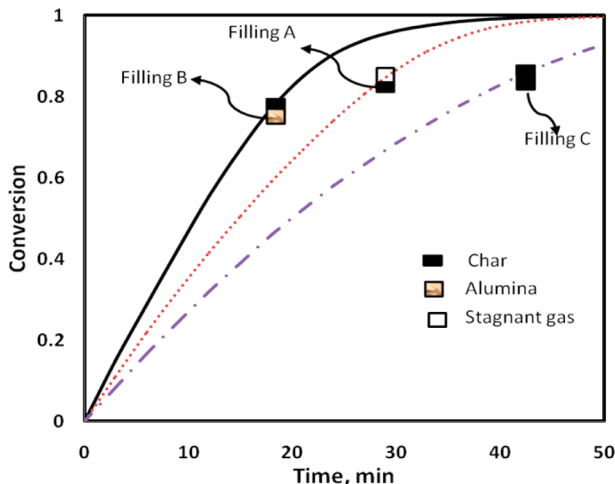


Figure 2. Comparison of conversion profiles for different crucible fillings in case of char B.

then cooled in an inert atmosphere and ground to a size less than 150 μm for further studies.

2.2. Demineralization of Coal and Ash Preparation. The grounded char is demineralized by acid washing.¹⁶ As explained later, gasification of the demineralized char is also studied to identify the catalytic effect, if any, of the ash present. Ash is obtained by the combustion of coal in an oxygen atmosphere at 975 K. The ash is analyzed by XRF and the composition of various important oxides is given in Table 3. The other major components not shown here are SiO₂ and Al₂O₃. Of particular interest here are the potassium compounds, as they are reported to be the most active catalytic species for gasification.

2.3. Procedure. The procedure to perform TGA experiments was standardized after carrying out several runs to ensure that we get reliable and consistent data on reaction kinetics. The reaction rate is also a strong function of how the char is prepared, and hence, an identical procedure of char preparation, described below, is followed in all the experiments:

- (1) The char sample is heated from ambient temperature to 110 °C at a rate of 30 °C/min in an inert nitrogen atmosphere with a flow rate of 150 mL/min. It was found that the effect of flow rate in this range is negligible, indicating that the external mass transfer limitations are absent.
- (2) The temperature is maintained for 30 min in order to dry the sample and to flush out air in the TGA chamber.
- (3) The temperature is then increased from 110 to 1000 °C at a rate of 30 °C/min and then kept constant for 10 min to ensure the completion of the pyrolysis reaction.
- (4) The sample is then cooled down to the reaction temperature (850–1000 °C) at a rate of 30 °C/min in the inert atmosphere.
- (5) The gasification of char with the reactive gas mixture (flow rate is 150 mL/min) is carried out at the desired temperature under isothermal conditions until the entire char is consumed.

The heterogeneous gas–solid reactions in the TGA involve, in addition to the intrinsic reaction, several transport processes:

- transfer of the gasifying agent and heat from the bulk gas to the external layer of the particle bed, i.e., external mass and heat transfer;
- diffusion of the gasifying agent and heat through the bed of char particles, i.e., intrabed mass and heat transfer; and
- diffusion of the gasifying agent and heat into the interior of the char particles (pore diffusion and effective conduction of heat through the porous particles).

When the char is ground to a very fine size, the pore diffusion resistance may be disregarded because of the short intraparticle diffusion path.⁴⁰ Further, it is possible that the kinetic data generated in TGA experiments may be influenced by diffusional effects. To illustrate this, we performed three different TGA experiments with different fillings of the crucible, as shown in Figure 2. The inner diameter of the crucible is 4 mm and the depth is 4.5 mm. For filling A, 10 mg of char is taken at the bottom of the crucible to examine the diffusion effect, if any, in the stagnant gas space. In filling B, a layer of 10 mg of char is placed above a bed of alumina, and in filling C, the complete

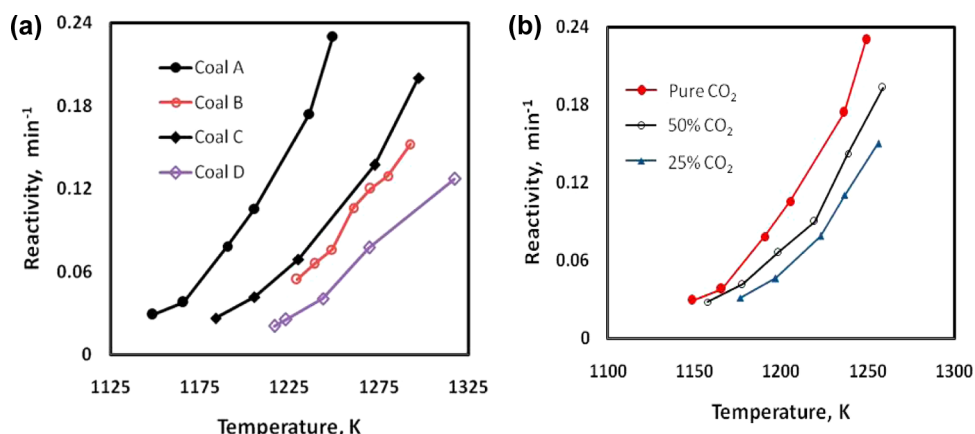


Figure 3. Char reactivity as a function of temperature. (a) Reactivity of all chars with pure CO₂. (b) Reactivity of char A for different partial pressure of CO₂ in a mixture with N₂.

crucible is filled with char. In all these cases, the gasification is carried out at a temperature of 1246 K. The conversion profiles are as shown in Figure 2. It can be seen that both the stagnant layer and bed diffusion effects are significant. To eliminate these

effects, the crucible should be filled with a minimum amount of char on the top of alumina, as in the case of filling B, giving highest rate, free of mass transfer limitations.

Hence, to obtain data close to intrinsic kinetics, all the gasification experiments, unless otherwise mentioned, are carried out by placing a layer of 2 ± 0.25 mg of char above a bed of alumina. The thickness of the char bed is typically 0.4 mm. The diffusional resistance of the bed is negligible for this thickness of the bed.⁴⁰ The CO₂ gasification experiments are carried out over a temperature range of 800–1050 °C, with pure CO₂ and at different reactant gas compositions with nitrogen as a diluent.

3. REACTIVITY OF DIFFERENT CHARS

The reactivity of char is an important property that governs its behavior in gasification processes. Several definitions are used to evaluate the reactivity of char. Gasification reactivity is quantified as⁴¹

$$\gamma(i) = \frac{dx_i/dt}{1 - x_i} \quad (2)$$

where x_i is the conversion of char at any time. The reactivity at 50% conversion is considered as the representative reactivity shown in Figure 3 for different char samples in this work.

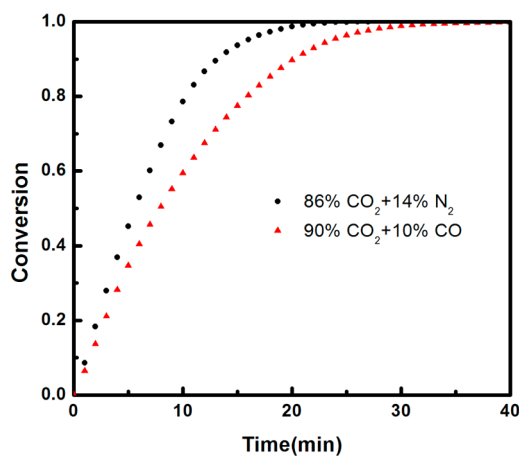


Figure 4. Experimental char conversion profiles indicating the effect of CO inhibition in CO₂ gasification, for char A.

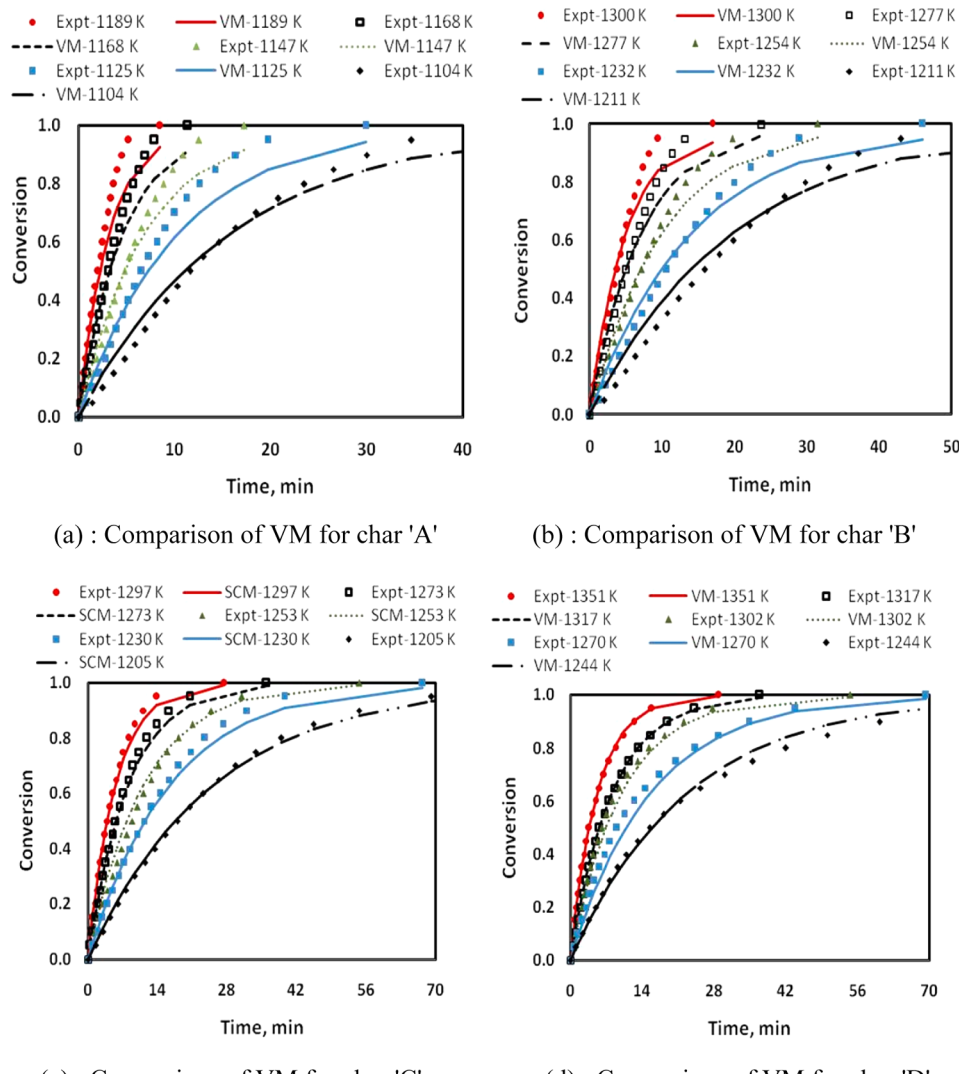


Figure 5. Comparison of conversion profiles predicted by the volumetric model with experimental conversions with pure CO₂ feed.

The comparison of reactivity of all the chars with pure CO₂ is shown in Figure 3a. Among the four chars used, Char A (low rank) is the most reactive and the char D has the least reactivity. The reactivity is highly sensitive to temperature and also depends on the partial pressure of the gasifying agent, which is indicated by Figure 3b for char A. As expected, with an increase in temperature and the partial pressure of CO₂, the reactivity of char increases. It is reported in the literature that the factors influencing the reactivity of char are mainly the rank of the coal,^{6,42} pyrolysis conditions such as the temperature and duration of pyrolysis,⁴³ and the heating rate.

4. KINETIC MODELING

Gasification experiments are carried out in the TGA using mixtures of CO₂ in nitrogen. To determine the inhibition effect of CO, which is a product of this reaction, gasification is also performed using mixtures of CO₂ and carbon monoxide.

For Indian lignite char (coal A) the conversion profile in CO₂ + N₂ atmosphere at 1126 K is compared with CO₂ + CO in Figure 4. Although the partial pressure of CO₂ is higher in the CO–CO₂ mixture compared to that in the N₂–CO₂ mixture, the reaction is relatively slow for the CO–CO₂ mixture. Hence, the inhibition due to CO is indeed significant. Such an effect is reported in

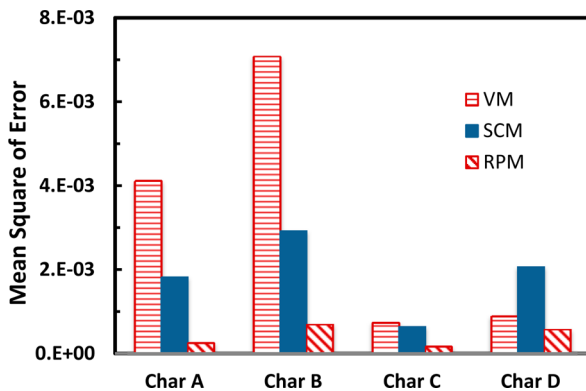


Figure 6. Comparison of mean square of error of three models for all chars.

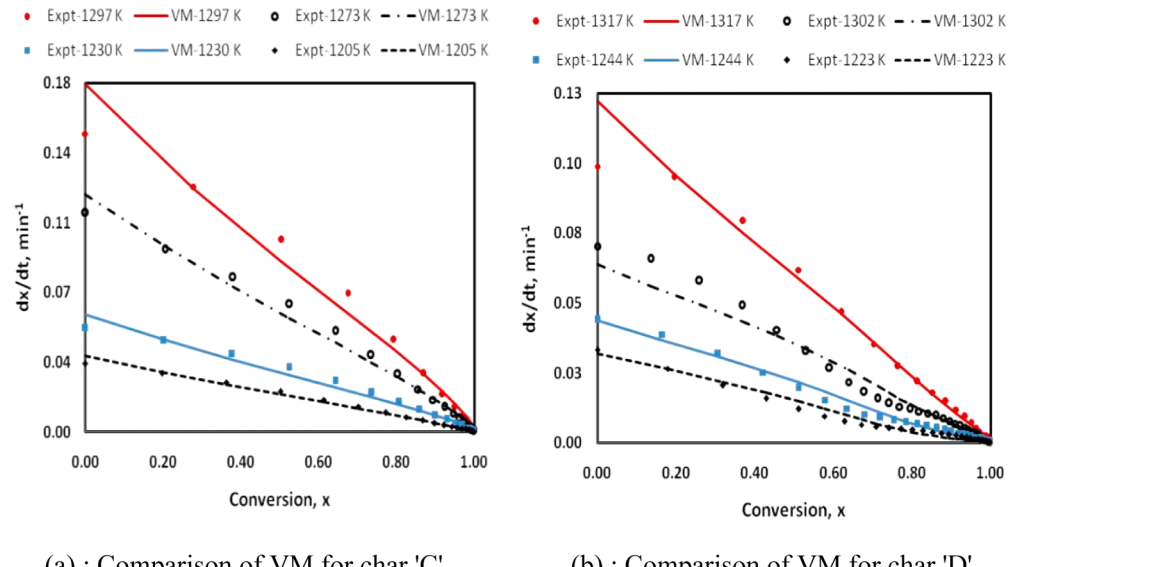
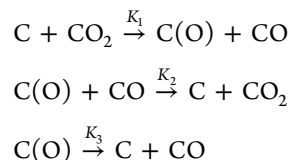


Figure 7. Comparison of conversion rate profiles of volumetric model predictions with the experimental data for pure CO₂ feed at different temperatures.

literature^{27,40–42,44–48} and the following mechanism is proposed for the same:



For kinetic modeling of CO₂ gasification of the chars, a simplified L–H rate equation is considered and it is given by²⁷

$$\frac{dx}{dt} = \frac{k_4 P_{\text{CO}_2}}{1 + K_5 P_{\text{CO}} + K_6 P_{\text{CO}_2}} f(x) \quad (3)$$

The values of k_4 , K_5 , and K_6 are calculated by fitting experimental data using multivariable linear regression. The adsorption coefficients of CO and CO₂ are assumed to be constant, while the temperature dependence of the reaction rate constant (k_4) is given by an Arrhenius expression

$$k_4 = k_0 e^{-E/RT} \quad (4)$$

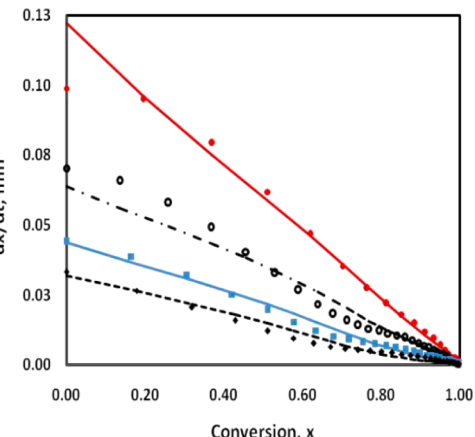
where k_0 and E are the pre-exponential factor and activation energy, respectively, and $f(x)$ is the relationship between reaction rate and conversion. Among the models shown in Table 1, three models are used in order to describe the gasification reaction of the char as they have a theoretical basis and fewer parameters involved. These are the volumetric model (VM),²⁸ the grain model (GM) or shrinking core model (SCM),²⁹ and the random pore model (RPM).³¹ The model parameters are estimated using *nlinfit* in MATLAB, which is based on the Levenberg–Marquardt algorithm.

4.1. Volumetric Model. This model assumes that a homogeneous reaction occurs throughout the char bed and that it results in a linear decrease in the reaction surface area with conversion. This model has been used for the gasification of different chars by several researchers.^{49–54} The overall reaction rate is given by

$$\frac{dx}{dt} = \frac{k_4 P_{\text{CO}_2}}{1 + K_5 P_{\text{CO}} + K_6 P_{\text{CO}_2}} (1 - x) \quad (5)$$

● Expt-1297 K — VM-1297 K ○ Expt-1273 K — VM-1273 K
■ Expt-1230 K — VM-1230 K ● Expt-1205 K — VM-1205 K

● Expt-1317 K — VM-1317 K ○ Expt-1302 K — VM-1302 K
■ Expt-1244 K — VM-1244 K ● Expt-1223 K — VM-1223 K



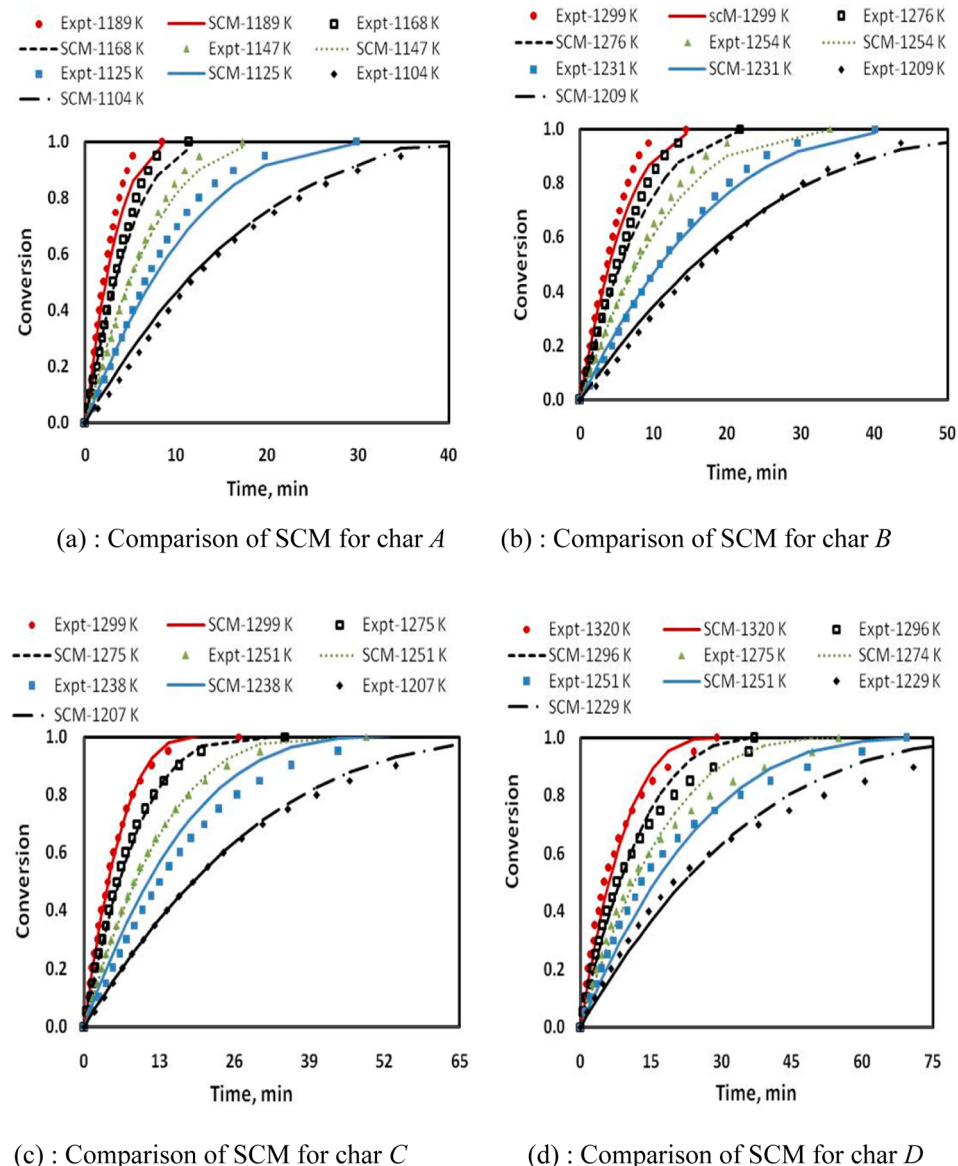


Figure 8. Comparison of shrinking core model predictions with the experimental conversions for 86% of CO_2 at different temperatures.

The conversion profiles predicted by the volumetric model are compared with experimental data in Figure 5 for a pure CO_2 feed. It is observed that the model predictions are in good agreement with the experimental data up to a limited conversion for chars A and B (e.g., ~50% for char A and 70% for char B). The mean square of errors (MSEs) between model predictions and experimental data for all the models are shown in Figure 6. In our work, for the other two chars, i.e., C and D, the model predictions of conversions are in good agreement (MSE value $<10^{-3}$) with the experimental data for the entire range of conversion, in line with the work of Adschari et al. (1986).⁵² The profiles of the conversion rate are shown in Figure 7, which indicate a good agreement with experimental data for these two chars. Thus, the volumetric model is applicable only for the chars C and D.

4.2. Shrinking Core Model. The GM or SCM, used by several researchers in the past,^{44,51,55–57} assumes that a porous particle consists of an assembly of uniform nonporous grains and the reaction takes place on the surface of these grains. The space between the grains constitutes the porous network. The shrinking core behavior applies to each of these grains during the reaction.

Assuming the reaction to be controlled by intrinsic kinetics and that the grains have a spherical shape, the overall reaction rate is given by

$$\frac{dx}{dt} = \frac{k_4 P_{\text{CO}_2}}{1 + K_5 P_{\text{CO}} + K_6 P_{\text{CO}_2}} (1 - x)^{2/3} \quad (6)$$

The model predictions are compared with the experimental data for all the coals, and the results are shown in Figure 8. The conversion profiles of SCM for char C are in good agreement with the experimental data. The conversion profiles in Figure 8 and the MSE values from Figure 6 indicate that this model is suitable for char C only.

4.3. Random Pore Model. The RPM model considers the overlapping of pore surfaces, which results in reduction in the surface area available for the reaction. It is known to be applicable to gasification and combustion of various coals. The general rate equation for this model is

$$\frac{dx}{dt} = \frac{k_4 P_{\text{CO}_2}}{1 + K_5 P_{\text{CO}} + K_6 P_{\text{CO}_2}} (1 - x) \sqrt{1 - \Psi \ln(1 - x)} \quad (7)$$

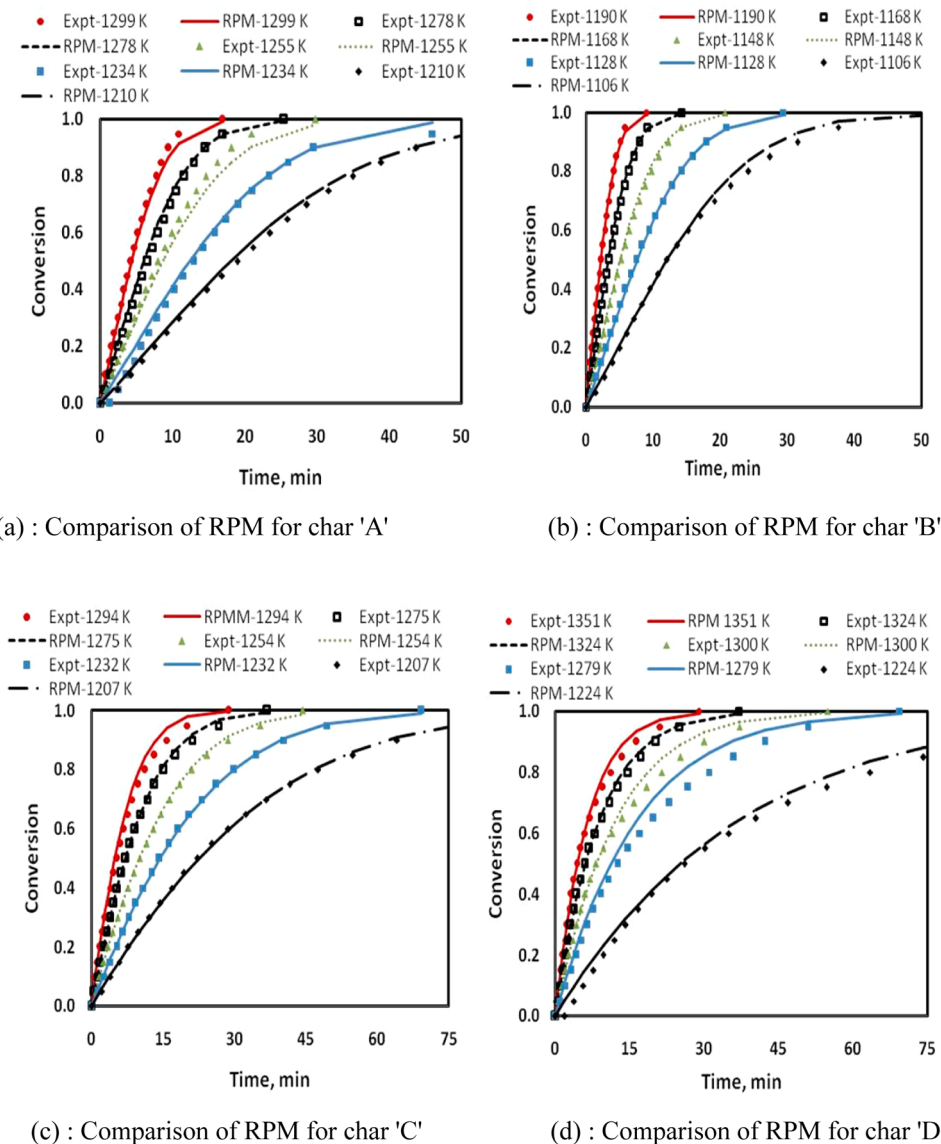


Figure 9. Comparison of prediction of RPM with experimental conversion data for 65% CO₂.

This model is able to predict a maximum for the reactivity as the reaction proceeds. This is because it considers the competing effects of pore growth during the initial stages of gasification and the destruction of the pores due to the coalescence of neighboring pores during the reaction. The RPM model contains two parameters, Ψ , which is related to the initial pore structure of the char sample ($x = 0$) and the reaction rate constant, k . The comparison of the model predictions with the experimental data for 65% CO₂ is shown in Figure 9. The conversion profiles and MSE for all the chars indicate a good agreement.

Figure 10 shows the comparison of conversion rate profiles with the experimental data for all the chars showing a good agreement. Hence, we conclude that among the three models used, the random pore model is the most appropriate and versatile model^{18,49,58–61} for predicting our experimental data. The estimated values of the model parameters of this model are listed in Table 4. The activation energies of coal chars is in the range 79–359 kJ/mol.⁴⁰ Among the four chars, the activation of energy for char D is significantly less than that of the other char samples.

Further, CO₂ gasification of all the demineralized chars (DMC) is carried out to determine the catalytic activity of mineral content in

the ash. It can be seen that the values of the activation energy for all the demineralized chars is around 230 kJ/mol. Clearly, it shows that the mineral matter in coal has a catalytic effect, which is also reported in the literature (e.g., see ref 9). It is also reported in the literature⁶³ that among the different ash components, potassium oxides have a strong catalytic effect toward gasification. Hence, the low activation energy of the char obtained from coal D can be attributed to the high ash content and potassium (K₂O is 0.36% in char), whereas char obtained from coal A, which has very low ash and potassium content, has higher activation energy, which is close to activation energy of demineralized char (K₂O is 0.01% in char).

5. BED DIFFUSION EFFECTS

In the case of underground coal gasification, we do not have control over the particle size, and hence the entire char is not directly exposed to the flowing gas. The gas will encounter diffusional resistance while the interior solid matrix of the char is accessed, and the overall rate of gasification is thus likely to be strongly influenced by this resistance. As described earlier in section 2, the TGA experiments suggest that there is significant diffusion resistance offered by the char bed. In this section,

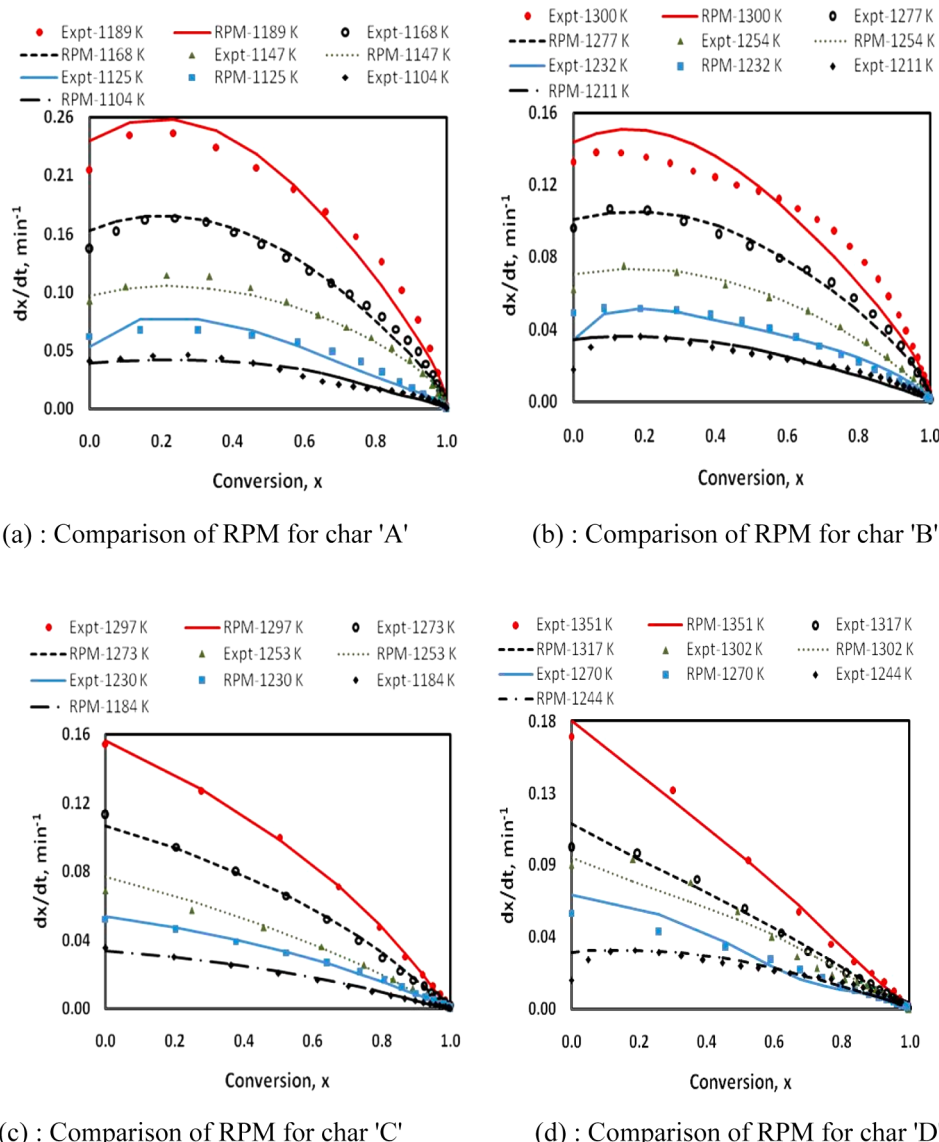


Figure 10. Comparison of prediction of RPM with experimental rates.

Table 4. Kinetic Parameters for the Random Pore Model with 95% Confidence Limit

	char A	char B	char C	char D
pre-exponential factor ($\text{atm}^{-1} \text{min}^{-1}$)	4.71×10^9	1.13×10^8	1.29×10^8	1.8×10^7
activation energy (kJ/mol)	229 ± 7	213.2 ± 6	215.1 ± 6.5	193 ± 6
K_6 (atm^{-1})	2.15 ± 0.13	1.17 ± 0.1	0.79 ± 0.05	2.32 ± 0.16
K_5 (atm^{-1})	0.83 ± 0.06	2.77 ± 0.15	0.79 ± 0.05	5.48 ± 0.3
model parameters	3.74 ± 0.1	3.187 ± 0.1	0.905 ± 0.01	0.147 ± 0.01
activation energy of demineralized char (kJ/mol)	229.1 ± 10	231.6 ± 9.5	228.9 ± 10	229.5 ± 10.5

we quantify this resistance through a one-dimensional reaction-diffusion model supported by several experiments conducted under different conditions. In these experiments the cylindrical crucibles are completely filled with char, as shown in Figure 11.

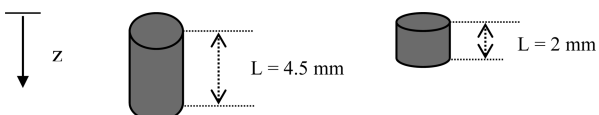
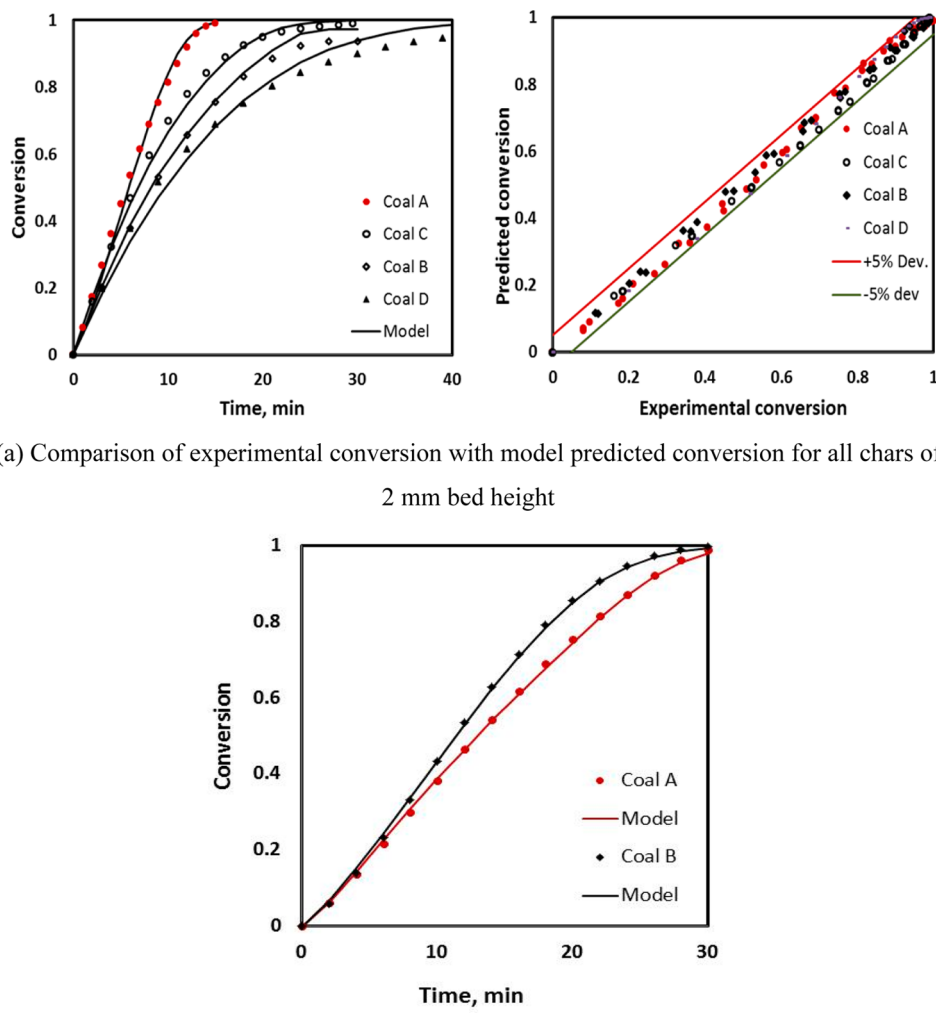


Figure 11. Crucible fillings for bed diffusion studies.

5.1. Assumptions. The developed model is based on the following assumptions:

- (1) It is a one-dimensional model and penetration of CO_2 through the bed in z direction is only diffusive.
- (2) During gasification, the bed is maintained at a constant temperature, and the temperature gradients in the bed are negligible. This is confirmed by independent simulations using representative bed conductivity values.⁶²
- (3) The gas is assumed to be ideal. Further, the total pressure remains constant throughout the bed.

**Figure 12.** Model predictions for 0.2 cm bed gasification.

- (4) The gas flux within the solid char bed is considered to be following Stefan's law of diffusion.
- (5) The random pore model is assumed to be applicable at local positions inside the bed.
- (6) The diffusivity in the char bed is assumed to be a linear function of char conversion or in other words, the bed diffusivity varies with time as carbon reacts.

The partial pressure of CO_2 (P_{CO_2}) and the density of coal (ρ_C) vary along the vertical position (z) within the bed and time (t).

5.2. Molar Balance of CO_2 . The molar balance of CO_2 is written as

$$\frac{dN_A}{dz} + \rho_{\text{CO}} \frac{dx}{dt} = \frac{dC_A}{dt} \quad (8)$$

where N_A is the molar flux of CO_2 and ρ_C is the molar density of the char.

For a multicomponent system, the molar flux of the species A can be written as

$$N_A = -CD_{\text{Ae}} \frac{dx_A}{dz} + x_A(N_A + N_B) \quad (9)$$

For the CO_2 gasification of char, $\text{C} + \text{CO}_2 \rightarrow 2\text{CO}$, the stoichiometry suggests that

$$N_B = -2N_A \quad (10)$$

where, N_B is the molar flux of CO. Further, by combining eqs 9 and 10, the molar flux for CO_2 is given by

$$N_A = -\frac{CD_{\text{Ae}}}{1 + x_A} \nabla x_A \quad (11)$$

For a one-dimensional system the above equation is reduced to

$$\begin{aligned} D_{\text{Ae}} \left\{ \frac{1}{1 + x_A} \frac{d^2 x_A}{dz^2} - \frac{1}{(1 + x_A)^2} \left[\frac{dx_A}{dz} \right]^2 \right\} - \frac{\rho_{\text{CO}}}{C} \frac{dx}{dt} \\ = \frac{dx_A}{dt} \end{aligned} \quad (12)$$

The boundary conditions for the eq 12 are at $z = 0$, $x_A = x_{\text{AG}}$ and at $z = L$, $dx_A/dz = 0$.

5.3. Mole Balance for Char. For the CO_2 gasification of char, the rate of consumption is

$$\frac{dx}{dt} = f(P_{CO_2}, P_{CO}, T) \frac{S_0}{1 - \varepsilon_0} g(x) \quad (13)$$

i.e.,

$$\frac{dx}{dt} = \frac{k_4 P_{CO_2}}{1 + K_S P_{CO} + K_6 P_{CO_2}} (1 - x) \sqrt{1 - \Psi \ln(1 - x)} \quad (14)$$

where $f(P_{CO_2}, P_{CO}, T)$ is a function that describes the dependency on partial pressure and temperature, and $g(x)$ represents the pore surface evolution during the carbon conversion. The values of parameters for the eq 14 are taken from Table 4. The initial condition for char consumption is at $t = 0, x = 0$.

The average conversion of char is given by

$$\bar{x} = \frac{1}{L} \int_0^L x \, dz \quad (15)$$

Equations 12 and 14 are solved along with the boundary conditions as specified.

5.4. Model Validation. The model eqs12 and 14 are discretized along the length of bed and solved using MATLAB ode23s solver. Diffusivity is assumed to be a linear function of conversion. The average conversion of the char is calculated by using eq 15. The simulations are carried out for different temperatures and for the two bed heights shown in Figure 11. The representative results for the 2 mm bed of different coals at the same temperature are shown in Figure 12. In Figure 12a the simulated results are compared with experimental conversion of all the coals for a bed of 2 mm, and Figure 12b compares the model with a single monolith cylindrical particle of 2 mm radius and 2 mm height for coals A and B. The parameters used for model simulations are shown in Table 5. These results are further

Table 5. Parameters for the Simulation of the Model

	temp (K)	diffusivity (m^2/s)	
		initial	final
char A	1142	3.3×10^{-6}	5.00×10^{-5}
char B	1325	6.67×10^{-6}	1.08×10^{-5}
char C	1320	2.17×10^{-5}	2.17×10^{-5}
char D	1325	2.17×10^{-5}	2.17×10^{-5}
char A monolith	1157	8.33×10^{-7}	4.57×10^{-5}
char B monolith	1257	8.3×10^{-6}	1.0×10^{-4}

validated by independent simulations performed in COMSOL. The assumption of isothermal conditions throughout the bed is validated by considering the heat of reaction in COMSOL.⁶² A two-dimensional model was considered and simulated for the temperature profiles within the bed. The observed temperature gradient in the bed is around 0.5 K, which is not significant. Hence, there are no heat transfer limitations for the particle sizes being considered. The results on monolith kinetics have a special significance, as one can extend the model for relatively large particles encountered in UCG, by incorporating the heat conduction effects, if any.

While, the constant diffusivity assumption is able to explain the experimental results for chars C and D, it is not valid for the other two types of chars. Simulations are also performed for the single monolith particle. It is observed that there is an order of magnitude difference between the initial and final diffusivities. Thus, this work indicates that for pulverized coals with high ash

content, it is acceptable to assume that the diffusivity remains constant during the gasification reaction.

6. CONCLUSIONS

The kinetics for CO_2 gasification of four different types of Indian coals was investigated in this work. Among these coals, the lignite, sample A, is found to be the most reactive. The coal reactivity varies in the order coal A > coal C > coal B > coal D. The experimental data on gasification kinetics obtained using the thermogravimetric analyzer for all the coals in this study are predicted well by the random pore model. TGA experiments carried out in the presence of CO indicate clearly the inhibition effect of CO on the gasification reaction. The activation energies for the gasification reaction of the coals are found to be 226 kJ/mol for coal A, 213 kJ/mol for coal B, 215 kJ/mol for coal C, and 193 kJ/mol for coal D. The lower value of activation for the coal D is due to the catalytic effect of ash and especially potassium oxide, which are present in large proportion. For the coals with small values of structural parameter Ψ , i.e., coals C and D, both the random pore model and volumetric models explain the data well. A one-dimensional reaction diffusion model is also developed for the gasification reaction in a packed coal bed by assuming a linear change of diffusivity within the bed. This model is able to explain the bed diffusion and kinetics of monolith particles of all the coals. Thus, the relevant parameters such as rate constants and diffusivities are successfully estimated for the coals of interest at conditions relevant to underground coal gasification. The kinetic model developed in the present work can be suitably incorporated in a global process model of UCG.

■ AUTHOR INFORMATION

Corresponding Author

*Phone: (022) 2576 7886. Fax: (022) 2572 4890. E-mail: aganesh@iitb.ac.in.

Notes

The authors declare no competing financial interest.

■ NOTATIONS

C	total molar concentration (mol m^{-3})
C_A	molar concentration of CO_2 (mol m^{-3})
D_{Ae}	effective diffusivity of CO_2 ($\text{m}^2 \text{s}^{-1}$)
E	activation energy (kJ mol^{-1})
k_4	Arrhenius rate constant ($\text{atm}^{-1} \text{s}^{-1}$)
K_S	adsorption coefficient of CO (atm^{-1})
K_6	adsorption coefficient of CO_2 (atm^{-1})
N_A	molar flux of CO_2 ($\text{mol m}^2 \text{s}^{-1}$)
N_B	molar flux of CO ($\text{mol m}^2 \text{s}^{-1}$)
P_{CO_2}	partial pressure of CO_2 (atm)
P_{CO}	partial pressure of CO (atm)
R	universal gas constant ($\text{J mol}^{-1} \text{K}^{-1}$)
S_0	initial surface area of char ($\text{m}^2 \text{gm}^{-1}$)
T	temperature (K)
k_0	pre-exponential factor ($\text{atm}^{-1} \text{s}^{-1}$)
n	dependency of rate on partial pressure
t	time (s)
x	conversion of char
\bar{x}	average conversion of char
x_A	mole fraction of CO ₂
x_{AG}	mole fraction of CO ₂ in gas phase
z	space (m)
ρ_{CO}	initial molar density of char (mol m^{-3})
ρ_C	molar density of char (mol m^{-3})

- ε_0 initial porosity of char
 ψ initial structural parameter of char

■ REFERENCES

- (1) Chao, C.; Edward, S. R. CO₂ control technology effects on IGCC plant performance and cost. *Energy Policy* **2009**, *37*, 915–924.
- (2) Yuso, O.; Jun, I.; Saburo, H.; Makoto, K.; Hiroaki, W.; Satoshi, U.; Hisao, M. Development of oxy-fuel IGCC system with CO₂ recirculation for CO₂ capture. *Energy Procedia* **2011**, *4*, 1066–1073.
- (3) Evgeny, S.; Arvind, V. Underground coal gasification: A brief review of current status. *Ind. Eng. Chem. Res.* **2009**, *48*, 7865–7875.
- (4) Muhammad, F. I.; Muhammad, R. U.; Kasukabe, K. Coal gasification in CO₂ atmosphere and its kinetics since 1948: A brief review. *Energy* **2011**, *36*, 12–40.
- (5) Ye, D. P.; Agnew, J. B.; Zhang, D. K. Gasification of a South Australian low-rank coal with carbon dioxide and steam: Kinetics and reactivity studies. *Fuel* **1998**, *77* (11), 1209–1219.
- (6) Beamish, B. B.; Karen, J. S.; Rodgers, K. A.; Jane, N. Thermogravimetric determination of the carbon dioxide reactivity of char from some New Zealand coals and its association with the inorganic geochemistry of the parent coal. *Fuel Process. Technol.* **1998**, *53*, 243–253.
- (7) Gaye, Ö. Ç.; Hayrettin, Y.; Gürüz, A. G. Physical and chemical properties of selected Turkish lignites and their pyrolysis and gasification rates determined by thermogravimetric analysis. *J. Anal. Appl. Pyrolysis* **2007**, *80*, 262–268.
- (8) Ocha, J.; Cassanello, M. C.; Bonelli, P. R.; Cukierman, A. L. CO₂ gasification of Argentinean coal chars: A kinetic characterization. *Fuel Process. Technol.* **2001**, *74*, 161–176.
- (9) Qinglei, S.; Wen, L.; Haokan, C.; Baoqing, L. The CO₂-gasification and kinetics of Shennmu maceral chars with and without catalyst. *Fuel* **2004**, *83*, 1787–1793.
- (10) Florindo, A. P.; Amorós, D. C.; Solano, A. L. CO₂–carbon gasification catalyzed by alkaline-earths: Comparative study of the metal–carbon interaction and of the specific activity. *Carbon* **1993**, *31* (3), 493–500.
- (11) Shufen, L.; Yuanlin, C. Catalytic gasification of gas-coal char in CO₂. *Fuel* **1995**, *74* (3), 456–458.
- (12) Amorós, D. C.; Solano, A. L.; Lecea, C. S. M. D.; Kapteijn, F. Assessment of the CO₂–carbon gasification catalyzed by calcium. A transient isotopic study. *Carbon* **1994**, *32* (3), 423–430.
- (13) Takashi, K.; Kazuhide, K.; Jianqin, C.; Hiromi, Y.; Akira, T. Combustion and CO₂ gasification of coals in a wide temperature range. *Fuel Process. Technol.* **1993**, *36*, 209–217.
- (14) Hiroyuki, O.; Toshimitsu, S. Mechanisms of CO₂ gasification of carbon catalyzed with group VIII metals. 1. Iron-catalyzed CO₂ gasification. *Energy Fuels* **1996**, *10*, 980–987.
- (15) Mühlen, H. J.; Sowa, F.; Van, H. K. H. Comparison of the gasification behaviour of a West and East German brown coal. *Fuel Process. Technol.* **1993**, *36*, 185–191.
- (16) Vincenzo, C.; Ljubisa, R. R. On the gasification reactivity of Italian sclcis coal. *Fuel* **1991**, *70*, 1027–1030.
- (17) Hao, L.; Chunhua, L.; Masaomi, T.; Shigeru, K.; Shigeyuki, U.; Toshinori, K.; Hiroaki, T. Mineral reaction and morphology change during gasification of coal in CO₂ at elevated temperatures. *Fuel* **2003**, *82*, 523–530.
- (18) Koichi, M.; Toru, Y.; Koji, K.; Yoshizo, S.; Akira, T.; Tomita, A. Transformation of alkali and alkaline earth metals in low rank coal during gasification. *Fuel* **2008**, *87*, 885–893.
- (19) Ying-Hua, H.; Hiromi, Y.; Akira, T. Gasification reactivities of coal macerals. *Fuel Process. Technol.* **1991**, *23*, 75–84.
- (20) Messenböck, R. C.; Dugwell, R. D.; Kandiyoti, R. Coal gasification in CO₂ and steam: Development of a steam injection facility for high-pressure wire-mesh reactors. *Energy Fuels* **1999**, *13*, 122–129.
- (21) Zhimin, H.; Jiansheng, Z.; Yong, Z.; Hai, Z.; Guanxi, Y.; Toshiyuki, S.; Massahiro, N. Kinetic studies of steam gasification of char in the presence of H₂, CO and CO₂. *Fuel* **1985**, *64*, 944–949.
- (22) Juan, A.; Jose, L. M.; Gavilan, J. M. Kinetics of lignite-char gasification by CO₂. *Fuel* **1985**, *64*, 801–804.
- (23) Turkdogan, E. T.; Vinters, J. V. Kinetics of oxidation of graphite and charcoal in carbon dioxide. *Carbon* **1969**, *7*, 101–117.
- (24) Everson, R. C.; Hein, W. J. P. N.; Kaitano, R.; Falcon, R.; Cann, V. M. D. Properties of high ash coal-chars derived from inertinite-rich coal: II. Gasification kinetics with carbon dioxide. *Fuel* **2008**, *37*, 3403–3408.
- (25) Yang, Y.; Watkison, A. P. Gasification reactivity of some Western Canadian coals. *Fuel* **1994**, *73*, 1786–1791.
- (26) Shufen, L.; Sun, R. Kinetic studies of lignite char pressurized gasification with CO₂, H₂ and steam. *Fuel* **1994**, *73*, 413–416.
- (27) Ollero, P.; Serrera, A.; Arjona, R.; Alcantarilla, S. The CO₂ gasification kinetics of olive residue. *Biomass Bioenergy* **2003**, *24*, 151–161.
- (28) Levenspiel, O. *Chemical Reaction Engineering*, 3rd ed.; Wiley: New York, 1998; pp 41–42.
- (29) Levenspiel, O. *Chemical Reaction Engineering*, 3rd ed.; Wiley: New York, 1998; pp 575–576.
- (30) George, R. G. A random capillary model with application to char gasification at chemically controlled rates. *AICHE J.* **1980**, *26* (4), 577–585.
- (31) Bhatia, S. K.; Perlmuter, D. D. A random pore model for fluid–solid reactions: I. Isothermal and kinetic control. *AICHE J.* **1980**, *26* (3), 379–386.
- (32) Bhatia, S. K.; Perlmuter, D. D. A Random pore model for fluid–solid reactions: II. Diffusion and transport effects. *AICHE J.* **1981**, *27* (2), 247–254.
- (33) Bhatia, S. K.; Vartak, B. J. Reaction of microporous solids: The discrete random pore model. *Carbon* **1996**, *34* (11), 1383–1391.
- (34) Srinivasalu, G. J.; Bhatia, S. K. A modified discrete random pore model allowing for different initial surface reactivity. *Carbon* **2000**, *38*, 47–58.
- (35) Kasaoka, S.; Sakata, Y.; Tong, C. Kinetic evaluation of the reactivity of various coal chars for gasification with carbon dioxide in comparison with steam. *Int. Chem. Eng.* **1985**, *25*, 160–165.
- (36) Dutta, S.; Wen, C. Y.; Belt, R. J. Reactivity of coal and char. 1. In carbon dioxide atmosphere. *Ind. Eng. Chem. Process Des. Dev.* **1977**, *16*, 1620–1630.
- (37) Anil, G.; Robert, F. Z.; Amir, R. Gasification kinetics of Western Kentucky bituminous coal char. *Ind. Eng. Chem. Process Des. Dev.* **1989**, *28*, 1767–1778.
- (38) Raghunathan, K.; Ray, Y. K. Y. Unification of coal gasification data and its application. *Ind. Eng. Chem. Process Des. Dev.* **1989**, *28* (5), 518–523.
- (39) Sateesh, D.; Ramesh, N. M.; Sanjay, M. M.; Anuradda, G.; Pal, A. K.; Sharma, R. K.; Preeti, A. Compartment modelling for flow characterization of underground coal gasification cavity. *Ind. Eng. Chem. Res.* **2011**, *50*, 277–290.
- (40) Ollero, P.; Serrera, A.; Arjona, R.; Alcantarilla, S. Diffusional effects in TGA gasification experiments for kinetic determination. *Fuel* **2002**, *81*, 1989–2000.
- (41) Zhimin, H.; Jiansheng, Z.; Yong, Z.; Hai, Z.; Guanxi, Y.; Toshiyuki, S.; Masahiro, N. Kinetic studies of char gasification by steam and CO₂ in the presence of H₂ and CO. *Fuel Process. Technol.* **2010**, *91*, 843–847.
- (42) Ye, D. P.; Agnew, J. B.; Zhang, D. K. Gasification of a South Australian low rank coal with carbon dioxide and steam: Kinetics and reactivity studies. *Fuel* **1998**, *77* (11), 1209–1219.
- (43) Hao, L.; Masahiro, K.; Chunhua, L.; Shigeru, K.; Toshinori, K. Effect of pyrolysis time on the gasification reactivity of char with CO₂ at elevated temperatures. *Fuel* **2004**, *83*, 1055–1061.
- (44) Tae-Wahn, K.; Sang, D. K.; Davi, P. C. F. Reaction kinetics of char-CO₂ gasification. *Fuel* **1988**, *67* (4), 530–535.
- (45) Philip, C. K.; Robert, G. S.; Normand, M. L. Char gasification by carbon dioxide: Further evidence for a two-site model. *Fuel* **1986**, *65* (3), 412–416.
- (46) Koenig, P. C.; Squires, R. G.; Laurendeau, N. M. Evidence for two-site model of char gasification by carbon dioxide. *Carbon* **1985**, *23* (5), 531–536.
- (47) Laurendeau, N. M. Heterogeneous kinetics of coal char gasification and combustion. *Prog. Energy Combust. Sci.* **1978**, *4*, 221–270.

- (48) Anthony, A. L.; Hong, J.; Ljubisa, R. R. On the kinetics of carbon (char) gasification: Reconciling models with experiments. *Carbon* **1990**, *28* (1), 7–19.
- (49) Murillo, R.; Navarro, M. V.; Lopez, J. M.; Garcia, T.; Callen, M. S.; Aylon, E.; Masatral, A. M. Activation of pyrolytic lignite char with CO₂: Kinetic study. *Energy Fuels* **2006**, *20*, 11–16.
- (50) Jung, S. L.; Sang, D. K. Gasification Kinetics of waste tire char with CO₂ in a thermo balance reactor. *Energy* **1996**, *21* (5), 343–352.
- (51) Wu, S.; Gu, J.; Li, L.; Wu, Y.; Gao, J. The reactivity and kinetics of yanzhou coal chars from elevated pyrolysis temperatures during gasification in steam at 900–1200 °C. *Process Saf. Environ. Protect.* **2006**, *84* (B6), 420–428.
- (52) Adschiri, T.; Tohru, S.; Toshinori, K.; Takehiko, F. Prediction of CO₂gasification rate of char in fluidized bed reactor. *Fuel* **1986**, *65*, 1688–1693.
- (53) Ashish, B.; Ram, B. J. V.; Rajeswararao, T. Kinetics of rice husk char gasification. *Energy Convers. Manage.* **2001**, *42*, 2061–2069.
- (54) Jaffri, G. R.; Zhang, J. Y. Catalytic gasification of Fujian anthracite in CO₂ with black liquor by thermogravimetry. *J. Fuel Chem. Technol.* **2007**, *35* (2), 129–135.
- (55) Shiyong, Wu.; Jing, G.; Xiao, Z.; Youqing, W.; Jinsheng, G. Variation of carbon crystalline structures and CO₂ gasification reactivity of Shenfu coal chars at elevated temperatures. *Energy Fuels* **2008**, *22* (1), 199–206.
- (56) Raymond, C. E.; Hein, W. J. P. N.; Henry, K.; Delani, N. Reaction kinetics of pulverized coal chars derived from inertinite rich coal discards: Gasification with carbon dioxide and steam. *Fuel* **2006**, *85*, 1076–1082.
- (57) Ahn, D. H.; Gibbs, B. M.; Ko, K. H.; Kim, J. J. Gasification kinetics of an Indonesian sub-bituminous coal-char CO₂ at elevated pressure. *Fuel* **2001**, *80*, 1651–1658.
- (58) Hao, L.; Chunhua, L.; Masahiro, K.; Shigeru, K.; Toshinori, K. Unification of gasification kinetics of char in CO₂ at elevated temperatures with modified random pore model. *Energy Fuels* **2003**, *17*, 961–970.
- (59) Jian, H. Z.; Zhi, J. Z.; Fu, C. W.; Wei, Z.; Zheng, H. D.; Hai, F. L.; Zun, H. Y. Modeling reaction kinetics of petroleum coke gasification with CO₂. *Chem. Eng. Process.* **2007**, *46* (7), 630–636.
- (60) Frederic, P.; Olivier, B.; Gerard, A. The effects of diffusional resistance on wood char gasification. *Process Saf. Environ. Protect.* **2008**, *86*, 131–140.
- (61) Tie-feng, L.; Yi-tian, F.; Yang, W. An experimental investigation into the gasification reactivity of chars at high temperatures. *Fuel* **2008**, *87*, 460–466.
- (62) Samdani, G. *Annual Progress Seminar Report*, 2011; IIT: Bombay, 2011.
- (63) Karimi, A.; Gray, M. R. Effectiveness and mobility of catalysts for gasification of bitumen coke. *Fuel* **2011**, *90*, 120–125.